

AD A091822

LEVEL

A083799

SC5202.9SA

4

GROWTH OF HgCdTe BY MODIFIED
MOLECULAR BEAM EPITAXY

12

SEMI-ANNUAL REPORT FOR PERIOD
1 MARCH 1980 THROUGH 31 AUGUST 1980

By

J. T. CHEUNG
Principal Investigator
(805) 498-4545

DTIC
SELECTED
NOV 18 1980

ROCKWELL INTERNATIONAL SCIENCE CENTER
1049 Camino Dos Rios
Thousand Oaks, CA 91360

Effective Date of Contract: 02/12/79
Expiration Date of Contract: 02/11/81

DISTRIBUTION STATEMENT A
Approved for public release
Distribution Unlimited

This research was sponsored by the Defense Advanced Research
Projects Agency under DARPA Order No. 3704, Contract No.:
MDA903-79-C-0188; monitored by Defense Supply Service.

The views and conclusions contained in this document are those of
the author and should not be interpreted as necessarily representing
the official policies, either expressed or implied, of the Defense
Advanced Research Projects Agency or the United States Government.

80 11 13 049



Rockwell International
Science Center

DDC FILE COPY

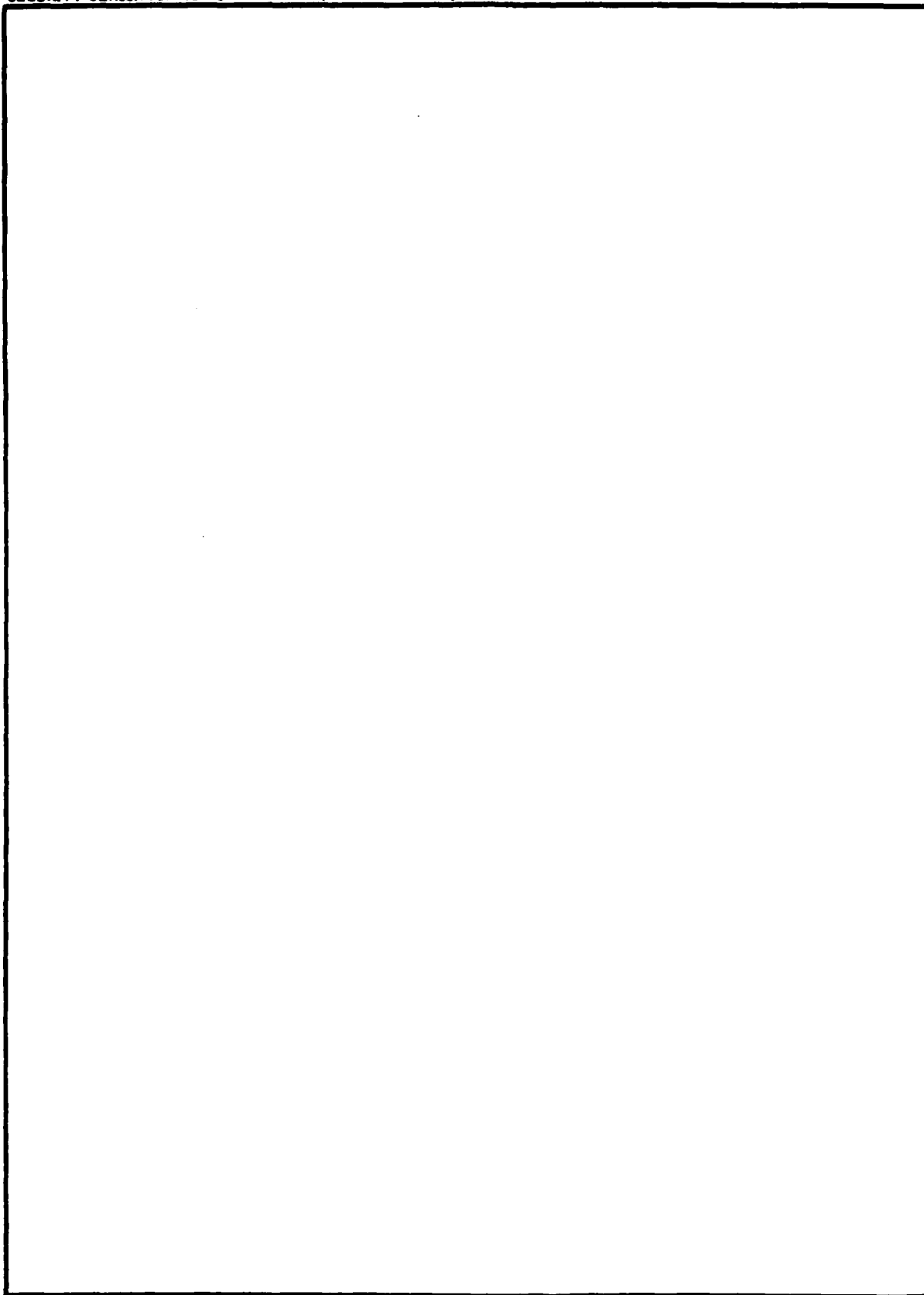
⑨ Semi-Annual Technical Rept. no. 3,
Unclassified 1 Mar - 31 Aug 89
SECURITY CLASSIFICATION OF THIS PAGE (When Data Entered)

REPORT DOCUMENTATION PAGE		READ INSTRUCTIONS BEFORE COMPLETING FORM
1. REPORT NUMBER	2. GOVT ACCESSION NO. AD-A091	3. RECIPIENT'S CATALOG NUMBER 822
4. TITLE (and Subtitle) GROWTH OF HgCdTe BY MODIFIED MOLECULAR BEAM EPITAXY.		5. TYPE OF REPORT & PERIOD COVERED Semi-Annual Technical (#3) 03/01/80 through 08/31/80
7. AUTHOR(s) J. T. Cheung		6. PERFORMING ORG. REPORT NUMBER SC5202.9SA
9. PERFORMING ORGANIZATION NAME AND ADDRESS Rockwell International Science Center 1049 Camino Dos Rios Thousand Oaks, CA 91360		8. CONTRACT OR GRANT NUMBER(s) MDA903-79-C-0188
11. CONTROLLING OFFICE NAME AND ADDRESS Defense Advanced Research Projects Agency 1400 Wilson Boulevard Arlington, VA 22209		10. PROGRAM ELEMENT, PROJECT, TASK AREA & WORK UNIT NUMBERS ✓ DARPA Order No. 3704
14. MONITORING AGENCY NAME & ADDRESS (if different from Controlling Office) 12 36		12. REPORT DATE October 1980
		13. NUMBER OF PAGES 35
		15. SECURITY CLASS. (of this report) Unclassified
		15a. DECLASSIFICATION/DOWNGRADING SCHEDULE
16. DISTRIBUTION STATEMENT (of this Report) Approved for public release; distribution unlimited.		
17. DISTRIBUTION STATEMENT (of the abstract entered in Block 20, if different from Report)		
18. SUPPLEMENTARY NOTES		
19. KEY WORDS (Continue on reverse side if necessary and identify by block number) HgCdTe, Epilayer, Laser Evaporation, Laser Annealing		
20. ABSTRACT (Continue on reverse side if necessary and identify by block number) HgCdTe thin films were deposited and annealed by laser radiation. The evaporants were analyzed by mass spectroscopy and their chemical compositions were found to depend on the laser scanning rate. The interaction of a short (10^{-7} sec) laser pulse with a crystalline HgCdTe surface was studied. Threshold values for inducing evaporation were determined to be 6×10^7 w/cm ² and 2×10^7 w/cm ² , respectively.		

10 to the minus 7
389949

Unclassified

SECURITY CLASSIFICATION OF THIS PAGE(When Data Entered)



Unclassified

SECURITY CLASSIFICATION OF THIS PAGE(When Data Entered)



Rockwell International
Science Center

SC5202.9SA

DISTRIBUTION

Director
Defense Advanced Research Projects
Agency
1400 Wilson Blvd.
Arlington, VA 22209

Attn: Program Management (2)
Attn: Dr. Richard A. Reynolds (1)

Defense Documentation Center
Cameron Station
Alexandria, VA 22314 (12)

Science Center Distribution:

J. T. Longo	(1)
D. T. Cheung	(1)
Group Secretary	(2)
Contracts & Pricing	(1)
Library	(1)
J. T. Cheung	(1)

Original +



SC5202.9SA

TABLE OF CONTENTS

	<u>Page</u>
SUMMARY.....	iv
1.0 INTRODUCTION.....	1
1.1 Program Objective.....	1
1.2 Overall Program Plan.....	1
1.3 Accomplishments.....	2
1.3.1 Apparatus Modification.....	2
1.3.2 Technical Achievements.....	3
2.0 TECHNICAL INFORMATION.....	5
2.1 Background.....	5
2.2 Experimental and Results.....	5
2.2.1 Splashing Effect.....	5
2.2.2 Evaporants Analysis Studies.....	12
2.2.3 Pulsed Laser Induced Melting and Resolidification Morphology on HgCdTe.....	19
2.2.4 Results on Laser Annealing.....	25
2.2.5 The Use of Pressed Powder Sample.....	28
3.0 FUTURE PLANS.....	29
4.0 REFERENCES.....	30

Accession For	
NTIS CRA&I	<input checked="checked" type="checkbox"/>
DTIC TAB	<input type="checkbox"/>
Unannounced	<input type="checkbox"/>
Justification	
By	
Distribution/	
Availability Codes	
Dist	
Special	



LIST OF FIGURES

	<u>Page</u>
Fig. 1 Angular dependence of the film thickness.....	8
Fig. 2 Angular dependence of the splashed micropenticle density.....	9
Fig. 3 Surface morphology with and without <u>in situ</u> laser annealing.....	11
Fig. 4 Mass spectrum of the evaporants (fast scan).....	13
Fig. 5 Mass spectrum of the evaporants (slow scan).....	14
Fig. 6 Surface temperature evolution after pulsed and CW laser irradiation.....	18
Fig. 7 Laser beam profile.....	21
Fig. 8 Surface morphology of an epilayer after laser annealing.....	22
Fig. 9 Surface morphology of a laser evaporated film before and after laser annealing.....	27



SC5202.9SA

SUMMARY

During the last six months period, we have up-graded the LADA apparatus by installing many new features, such as the liquid nitrogen cooled cryo-panel, a pair of x-y optical scanners and a Hg source to provide a Hg back pressure in the vacuum chamber. These modifications are based on the need of the system and are expected to improve the performance.

Technically, we have completed the study of laser induced evaporation using mass spectroscopy. We have also examined the problem of splashing micro particles onto substrate during laser evaporation and devised solutions. Finally, we studied the laser annealing process on HgCdTe. Some unexpected results due to rapid resolidification will be presented.



SC5202.9SA

1.0 INTRODUCTION

1.1 Program Objective

The main objective of this program is to explore and develop a novel epitaxial technique for the growth of HgCdTe system. The process is named LADA. It combines the use of laser evaporation and in situ laser annealing. Potentially, this technique can be applied to many other materials.

1.2 Overall Program Plan

Due to the pioneering nature of the subject, the program plan was divided into three phases. Work in Phase I involves equipment purchasing, system design and construction. Experimental work started in Phase II. These experiments served two purposes, to discover the design flaws of the apparatus and to provide guidance for modification. In addition, they were used to study the fundamental properties such as the growth rate, the stoichiometric control, and the laser annealing processes etc. Once a routine operation is established, we will start Phase III. The purpose of the final phase is growth optimization and material characterization. Our current activities have been mainly involved with the work in Phase II with some ventures into Phase III.



SC5202.9SA

1.3 Accomplishments

The accomplishments during this six-months period can be divided into the areas of apparatus modification and technical achievements.

1.3.1 Apparatus Modification

We have modified the LADA apparatus by the following additions:

- A. The addition of two liquid nitrogen cooled panels inside the vacuum chamber. One panel located just behind the substrate holder and the other one is around the source holder. These cryo-panels trap the uncondensed beam particles to prevent multiple collisions.
- B. We have installed and aligned two sets of x-y galvanometric mirror scanners. They are used for scanning the laser beams over the substrate and source surfaces for annealing and evaporation respectively.
- C. We have installed a heated quartz plate just in front of the vacuum laser window to prevent the window clouding during evaporation. This provides a temporary solution to the problem.
- D. We have installed a Hg source which is isolated from the main chamber through a valve. Its temperature can be regulated to



SC5202.9SA

supply a back pressure of Hg ranging from 10^{-2} torr to 10^{-6} torr in the main chamber during evaporation.

1.3.2 Technical Achievements

- A. We have analyzed the chemical identity of the evaporants by using mass spectroscopy under different laser scanning rates. The results can be interpreted in terms of the slow cooling rate of this material.
- B. We have studied the effect of splashing micron size molten particles onto the substrate during laser evaporation. Solutions to this problem were devised.
- C. We have studied the interaction of a high power laser with a crystalline HgCdTe surface systematically. Three types of interactions were identified. They are: vaporization, slow solidification and rapid solidification.
- D. We have studied the effects of laser annealing on HgCdTe thin films both after and during (in situ) deposition. The laser annealed sample showed a surface with features typical of the condensation from liquid phase. In one case, the surface showed triangular line pattern characteristics of the $\langle 111 \rangle$ crystal



SC5202.9SA

orientation. This was also verified by Laue x-ray reflection measurements.

- E. We have used pellets of HgTe and CdTe powder mixture as evaporation source material. The film quality is harder to control than by using bulk sources. There is an excessive amount of splashing.



SC5202.9SA

2.0 TECHNICAL INFORMATION

2.1 Background

In the last semi-annual report, we pointed out that the two most severe obstacles in depositing thin HgCdTe film by laser pulse were the splashing of the source material and the control of a congruency evaporation. Our efforts in this six-month reporting period were aimed toward solving these problems.

Another area which needs improvement is to develop a new source of evaporating materials. At the start of the program, we evaporated slices of bulk HgCdTe. However, this is not a practical choice because bulk material is costly, not readily available and does not have the flexibility in composition adjustment. We choose the cold-pressed homogenized powder mixture of HgTe and CdTe as an alternative.

2.2 Experimental and Results

2.2.1 Splashing Effect

When a laser beam with sufficient energy impinges on a solid surface, it vaporizes the surface substrate into atoms, molecule and molecular clusters. If the power level is very high, the surface can also erupt with hot solid particles and/or molten droplets. This phenomenon is known as the "splashing effect."¹ The resultant film shows extremely poor morphology and



SC5202.9SA

crystalline quality. High speed photographic study of the laser generated plume showed that such microparticles were ejected with a velocity of approximately 10^6 cm/s. These impacts could induce damage in the film.²

Splashing occurs when the sub-surface material is heated above its boiling point before the surface material is completely vaporized. Under such circumstances, the remainder of the top surface material can explode in the form of small particles. A common solution to avoid this problem is to lower the laser power and reduce the pulse width. By lowering the peak power, the surface temperature is lowered and the reduction of the pulse width limits the depth of the heat penetration. Such practice would meanwhile drastically reduce the evaporation rate and therefore not practical.

There are two viable approaches to minimizing this problem. They are the use of proper source-substrate geometric arrangement and the use of in situ laser annealing.

In almost all the previous work on the thin film growth laser evaporation, the substrates located very close to the laser beam. We found that this arrangement is most susceptible to the splashing. An off-axis mounting will be much better. When the sub-surface superheats, the microparticles leave the surface with a very high velocity in the direction normal to the surface. The velocity components parallel to the surface are much slower. The large differences in these velocity vectors tend to confine the microparticles within a small cone around the normal. The lighter evaporated species such as atoms, molecules and clusters have higher lateral



SC5202.9SA

velocity components, thus wider angular distribution. If the substrate is placed outside the central cone yet still intercepting the evaporated molecules and clusters, the splashing effect can be avoided.

A simple experiment was performed to verify this prediction. A number of polished substrates were placed at equal distance to the evaporation source on a circular holder. After 30 minutes of deposition, with high power laser pulses (7×10^7 W/cm², 1500 Hz, 100 n sec), the film thickness were measured and the microparticle densities on the surfaces were counted. Their angular dependence should reflect the spatial distribution of the atoms (molecules and clusters) and the micro-particles in the evaporants respectively. The results are shown in Fig. 1 and Fig. 2. The angular distribution of the film thickness (i.e., the atomic, molecular and cluster species) has a $\langle \cos^3 \theta \rangle$ dependence while the angular distribution of the splashed particles shows a $\langle \cos^8 \theta \rangle$ distribution and indeed they concentrate more near the normal. Therefore we can place the substrate at some angle off the normal axis to avoid the splashing. For example, in this case, the splashing effect can be nearly eliminated by placing the substrate at 45° from the normal. The trade-off is a four-fold reduction in the deposition rate. The proper choice of the substrate location varies for different laser conditions. The compositional uniformity of the evaporants at various angles should also be examined.

In addition to the above approach, we also found that the splashed particles can be removed effectively by in situ laser annealing. The adhesion of the splashed particles to the substrate surface is very weak. Therefore,



Rockwell International
Science Center

SC5202.9SA

SC80-9254

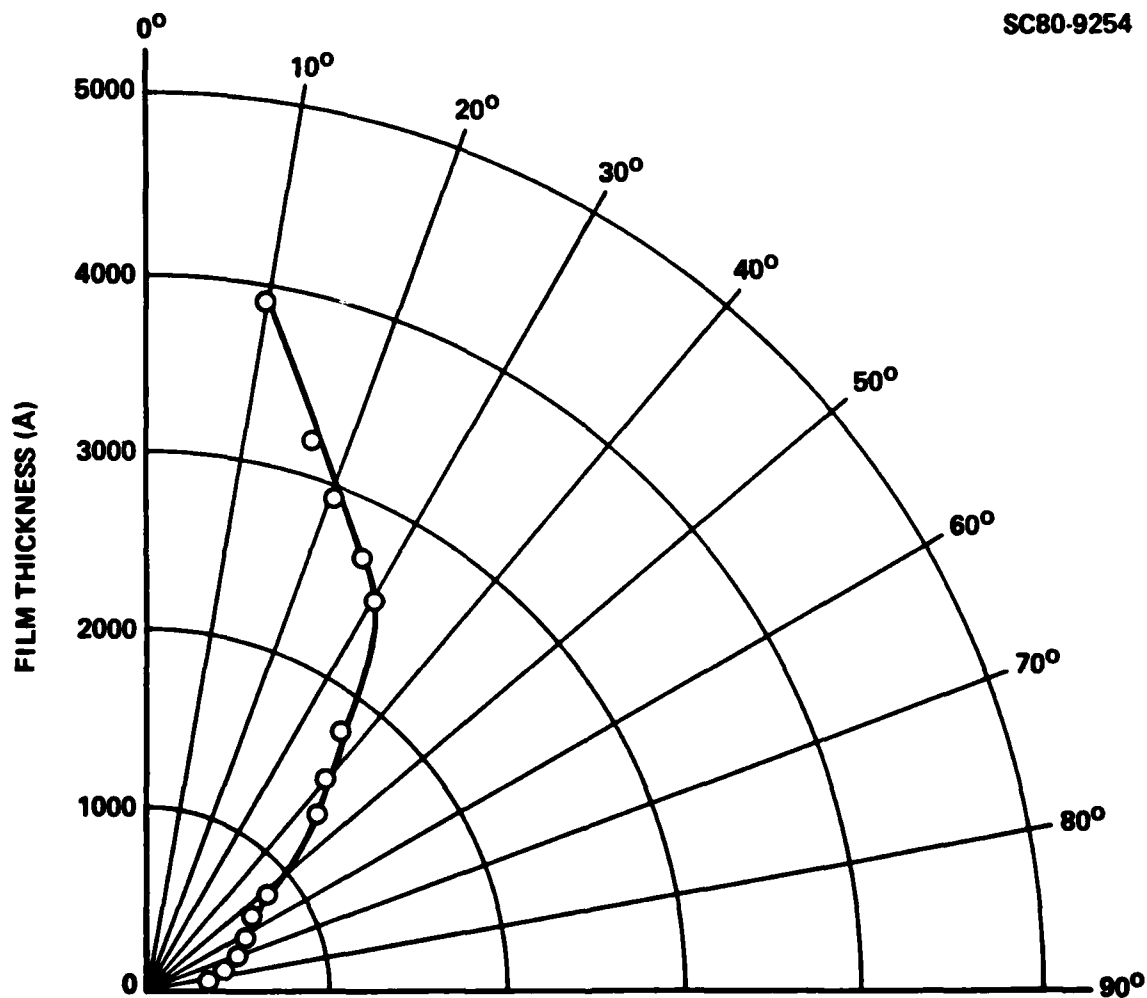


Fig. 1 Angular dependence of the film thickness.



SC80-9255

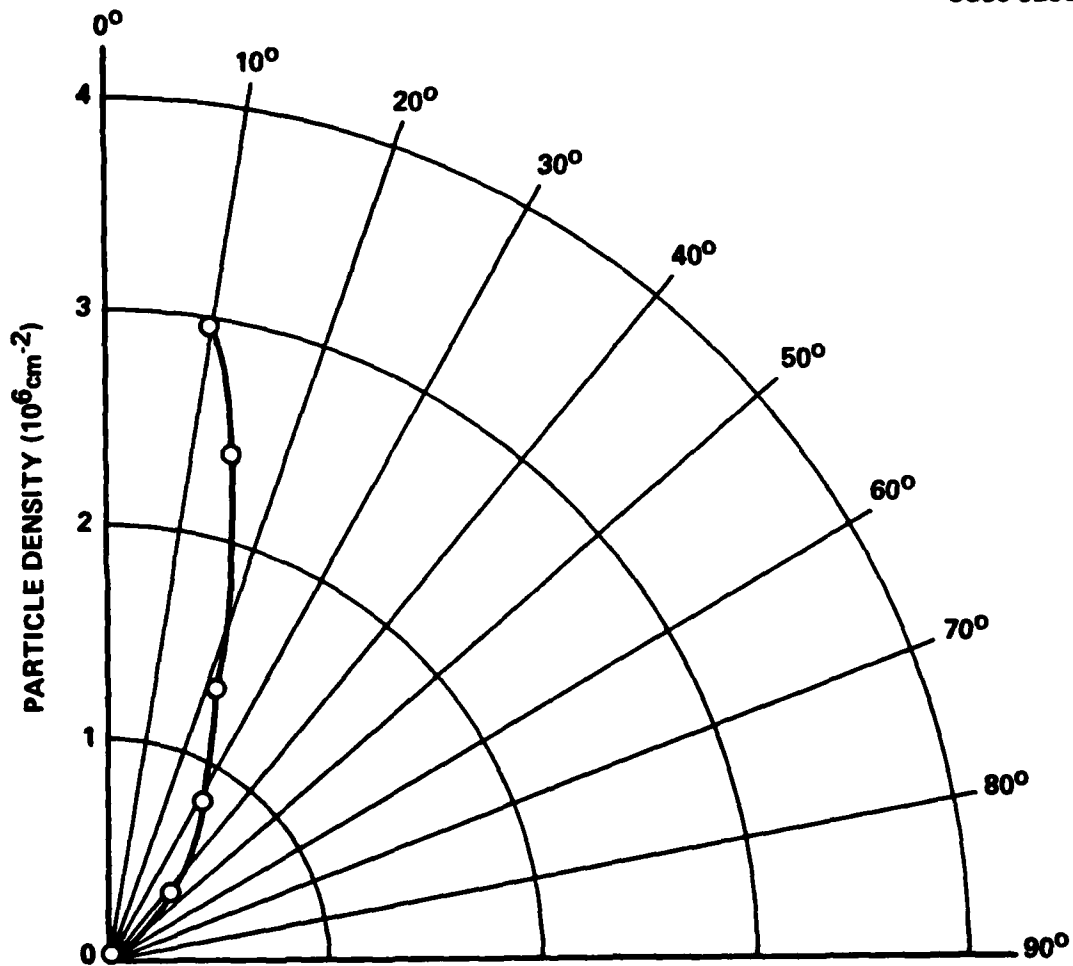


Fig. 2 Angular dependence of the splashed microparticle density.

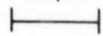


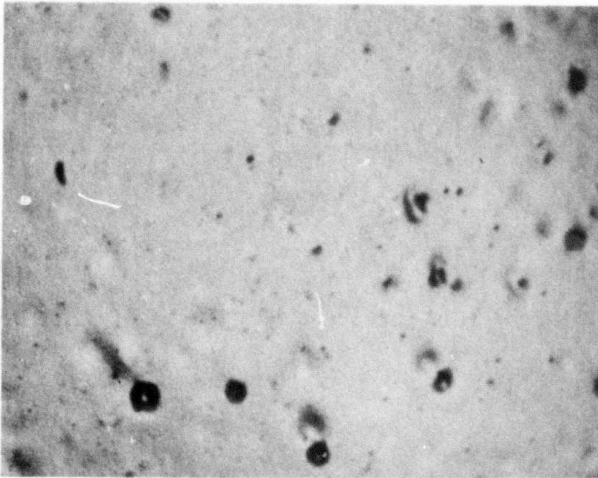
SC5202.9SA

when the substrate is scanned with medium power ($\sim 10^7$ W/cm²) laser pulses, the energy absorbed at the interface between the particle and the substrate surface is sufficient to remove these particles. An example is given in Fig. 3. It shows the surfaces of two different areas on the same film with (Fig. 3a) and without (Fig. 3b) in situ laser annealing. The laser pulses were defocused to a spot 0.3 mm in diameter. At the edge of this circular region the power density is 10^7 W/cm². The beam has a pulse frequency of 6 kHz with pulse width of approximately 150 nsec. The in situ annealing beam was directed onto the substrate intermittently by a mirror mounted on a rotating wheel. The details were described in our last semi-annual report. The area without in situ laser annealing shows a large density of splashed particles. On the area with in situ laser annealing, the surface is much smoother. Most of the splashed particles were removed. There are still particles left on the surface, some of them are half buried. We believe that it is due to the optical arrangement. Since the mirror which directs the laser beam onto the substrate for annealing is mounted on a rotating wheel, the substrate surface is only exposed to the laser radiation for short intermittent intervals. In the present setup, the mirror intercepts the laser beam for laser annealing once every 30 seconds. Each annealing process lasted about 2 seconds which was too short for the laser beam to be scanned over the entire area of 3/4 inches and 1 inch. Therefore, there were be some "dead" areas. Splashed particles in this area did not experience the annealing laser pulses and were buried by the arrival of more evaporants. In order to circumvent this problem, in situ laser annealing has to be carried out

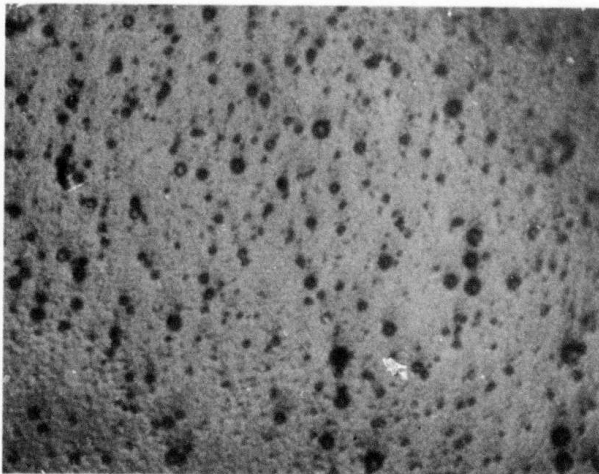


SC80-10586

10 μm




(a) WITH IN SITU LASER ANNEALING



(b) WITHOUT IN SITU LASER ANNEALING

Fig. 3 Surface morphology with and without in situ laser annealing.



SC5202.9SA

continuously during the deposition process. We have replaced the rotating mirror with a fixed beam splitter. The surface of the beam splitter is coated for 70% transmission and 30% reflection at 1.06 μm wavelength. Power density of the in situ annealing laser beam can be adjusted independently by focussing and defocussing the lens. Experiments with the new arrangement will be carried out shortly.

2.2.2 Evaporants Analysis Studies

In the previous semi-annual report, we reported the results of a mass spectroscopic analysis of the evaporants during a slow laser scan. Our results indicated the presence of a large amount of free Hg atoms. We reasoned that the production of free Hg atom was due to the accumulation of heat during a slow scan. We speculated that if the pulse rate was high enough such that there is no overlap of laser pulses, then the generation of free Hg atoms would be greatly reduced.

To verify this prediction, we installed a galvanometric mirror scanner to scan the beam over the source surface. We measured the mass spectrum of the evaporants when the scanner was operated at the highest attainable frequency (~ 100 Hz). The mass spectrum under this condition is shown in Fig. 4. The previous result is included in Fig. 5 for comparison. Indeed, the fast laser scan generates evaporants with a lower free Hg content.



Rockwell International
Science Center
SC5202.9SA

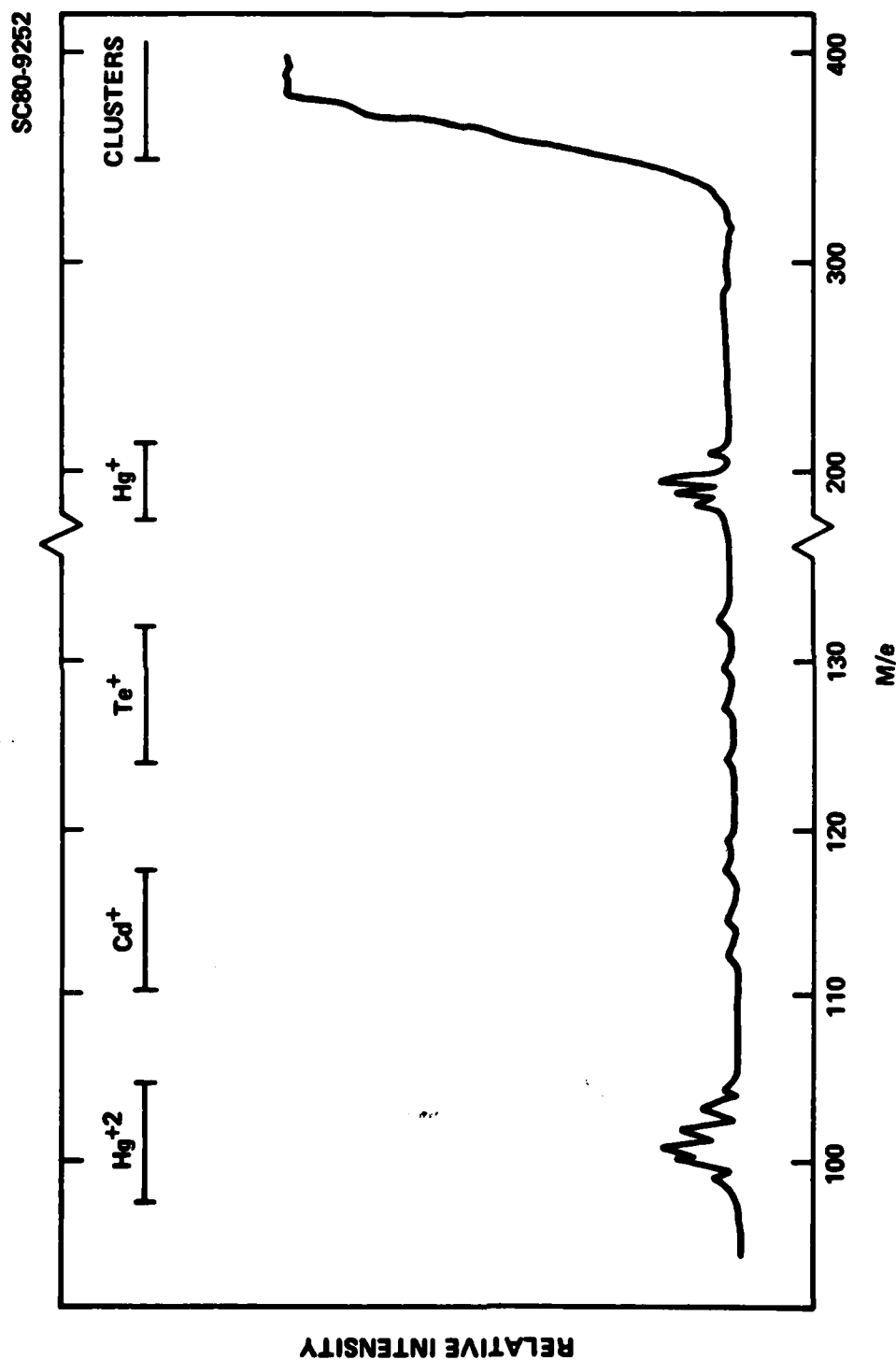


Fig. 4 Mass spectrum of the evaporants (fast scan).

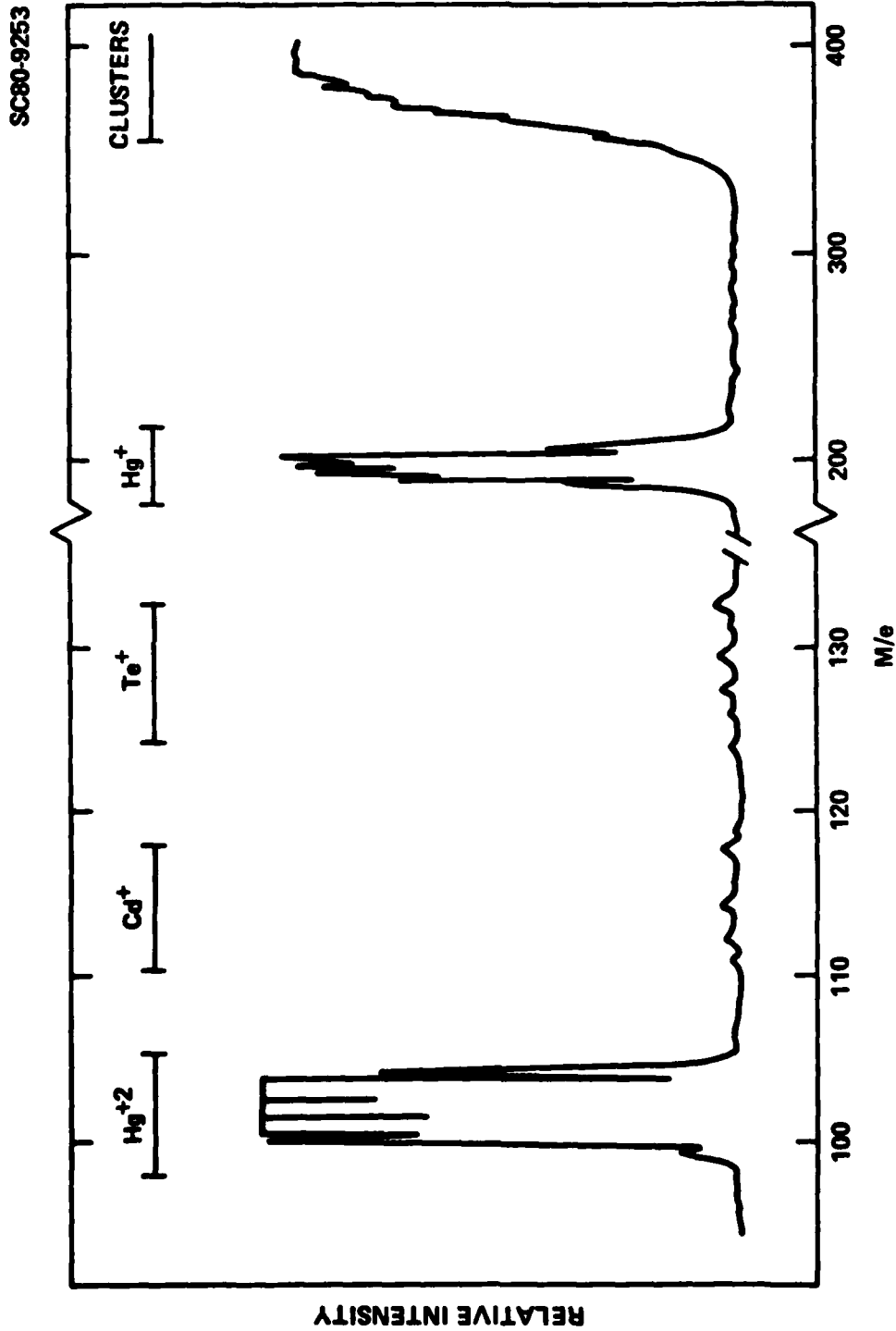


Fig. 5 Mass spectrum of the evaporants (slow scan).



SC5202.9SA

In order to obtain some quantitative insight of this problem, we made an effort to calculate the temperature of HgCdTe surface after the irradiation of a 100 ns duration laser pulse.

Temperature rise due to laser heating can be calculated by solving the differential equation for heat flow. If we limit ourselves to a single material phase, the following assumptions can be made to simplify the problem:

- A. The heat flows in one-dimension from the surface to the interior.
- B. Neglect the blackbody radiation loss and ignore the latent heat associated with a phase transition.
- C. All physical constants are temperature independent.

Under these conditions, the differential equation for heat flow into the interior with a boundary at $x = 0$ is:

$$\frac{\partial^2 T(x,t)}{\partial x^2} - \frac{1}{K} \frac{\partial T(x,t)}{\partial t} = - \frac{A(x,t)}{K} \quad (1)$$



SC5202.9SA

where T is the temperature, t the time after the turn-on of the laser pulse, k the thermal diffusivity, K the thermal conductivity and A is the radiation power density per unit time. The initial and boundary conditions are:

$$\begin{aligned} T(x,0) &= 0 \\ T(x,t) &\rightarrow 0 \quad \text{as } x \rightarrow \infty \end{aligned} \quad (2)$$

For a step source (such as the turn-on of a CW laser):

$$\begin{aligned} A(x,t) &= 0 & \text{for } t < 0 \\ A(x,t) &= (I - R)I_0 e^{-\alpha x} & \text{for } t > 0 \end{aligned} \quad (3)$$

where R is the reflectivity, I_0 is the power density and α is the absorption coefficient. The solution of Eq. (1) can then be expressed in terms of the complementary error function (erfc) and its integral (ierfc):



SC5202.9SA

$$\begin{aligned}
 T(x,t) = & (1 - R) (2I_0/K)(kt)^{1/2} \operatorname{ierfc} [x/2(kt)^{1/2}] - I_0 e^{\alpha x}/K\alpha \\
 & + (I_0/2K\alpha) e^{\alpha^2 kt - \alpha x} \operatorname{erfc} (kt)^{1/2} \alpha - [x/2(kt)^{1/2}] \\
 & + (I_0/2K\alpha) e^{\alpha^2 kt + \alpha x} \operatorname{erfc} (kt)^{1/2} \alpha + [x/2(kt)^{1/2}] \quad (4)
 \end{aligned}$$

For pulsed operation, the laser pulse can be approximated by a number of successive steps and the solution corresponds to the superimposition of Eq. (4). Using HgCdTe as an example, $R = 0.3$, $\alpha = 10^{-4} \text{ cm}^{-1}$, $K = 0.1 \text{ W/cm} - \text{K}^\circ$, $k = 0.09 \text{ W cm}^2/\text{s}$. We have calculated the surface temperature evolution for both the CW ($6 \times 10^4 \text{ W/cm}^2$) and pulsed ($5 \times 10^7 \text{ W/cm}^2$) radiation. The power density quoted here is typical in our experiments. The 200 ns duration pulse is replaced with a three step approximation. The results are shown in Fig. 6. The pulsed radiation produces very high surface temperature with rapid heating and cooling rate. The fast cooling rate indicated by the calculation disagrees with our reasoning about the mass analysis of the evaporation. According to the calculation, the surface temperature cools down to 300°K in the period of time as short as 0.1 ms after the laser pulse. If so, the heat accumulation due to overlapped pulses at a few thousand Hz should not occur. We think that the discrepancy is in the

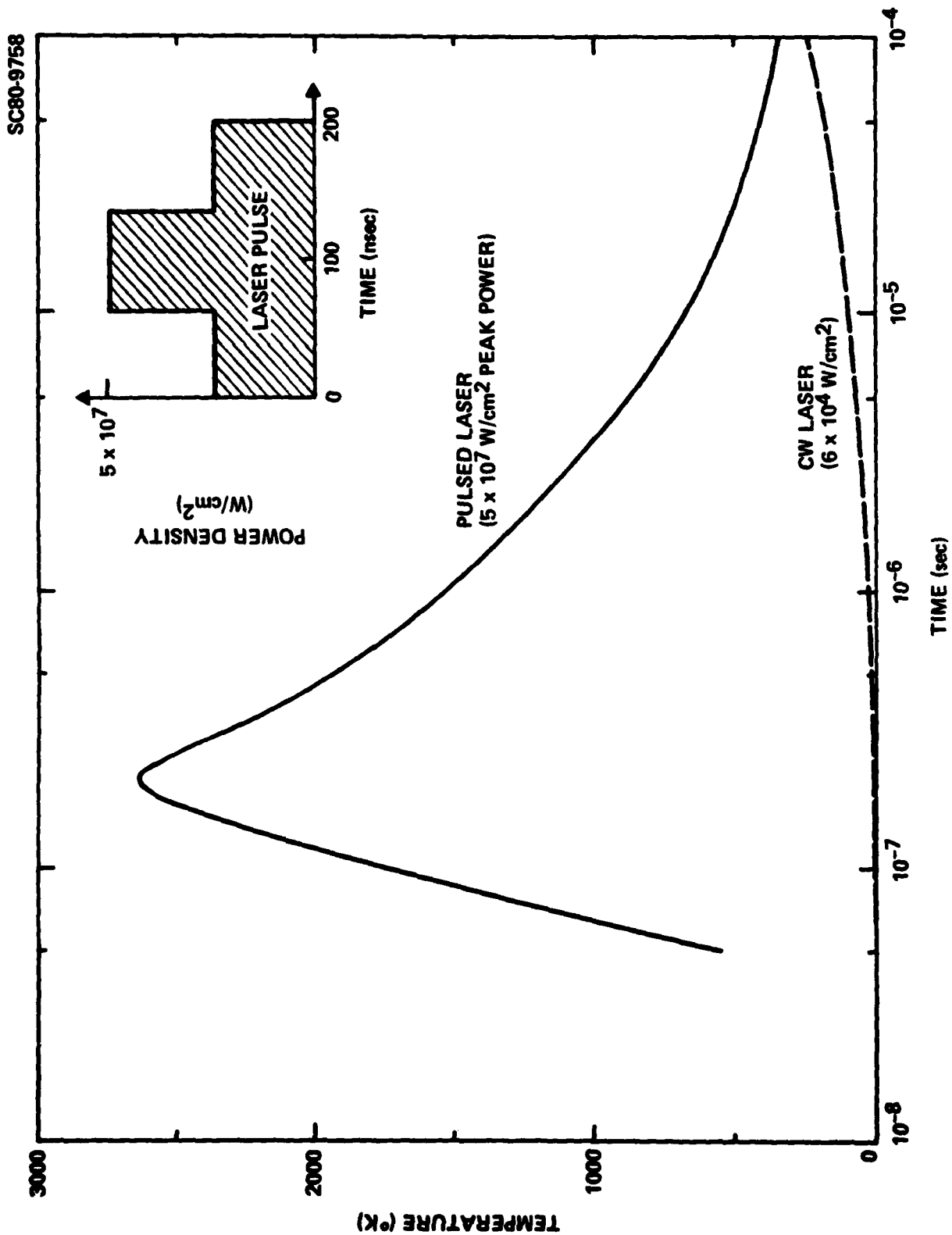


Fig. 6 Surface temperature evolution after pulsed and CW laser irradiation.



SC5202.9SA

over simplification of the calculation, because the assumption of constant physical parameters is no longer valid after the surface temperature exceeds the melting point.

2.2.3 Pulsed Laser Induced Melting and Resolidification Morphology on HgCdTe

Our work requires an extensive knowledge on the interaction of laser radiation with a HgCdTe surface. For example, the threshold values of power density for melting and evaporation can be very useful. Unfortunately, such information is very sparse in open literature. The only work which is remotely related to the subject is a series of experiments by Bantoli in a study of laser damage to HgCdTe photoconductive detectors. In these experiments, they measured the laser power for the onset of damaging a HgCdTe photoconductor. Pulses with various durations from a 10.6 μm CO_2 laser were used. For a 10^{-7} s pulse, the threshold value was about 10^7 W/cm^2 . However, their work dealt only with the detector performance before and after the laser irradiation. The morphological change was overlooked.

This prompts us to carry out a systematic study on the laser-surface interaction under a normal LADA condition. Short (10^{-7} s) high power radiation can cause fast heating and cooling rate up to 10^9 $^\circ\text{C}/\text{s}$. For a compound semiconductor material, such a HgCdTe, it is possible that the system cannot readjust itself to an equilibrium state in such a short time and therefore it may lead to a new kind of phase transition kinetics. For example, as shown in Section 2.2.2, the evaporation under this condition is not an equilibrium



SC5202.9SA

process. In this section, evidence is presented that a single crystal HgCdTe surface may be transformed into an amorphous layer, following melting induced by a short pulse.

In our experiments, a Q-switched Nd²⁺:YAG system produced pulses with an average duration of 200 ns at 10.6 μm wavelength. The laser beam was focused onto the sample surface after a 5 to 1 beam expansion. Average power and the pulse shape were measured with a factory calibrated photodiode. The beam profile, shown in Fig. 7, was measured by moving a 25 μm diameter pinhole in front of the photodetector at the focal plan. The beam shape is Gaussian with a FWHM of 80 μm . Samples used for irradiation were 20 μm thick Hg_{0.8}Cd_{0.2}Te grown by LPE technique on <111> CdTe substrates. The beam scanning rate was adjusted such that the pulse to pulse distance was about 80 μm . In other words, there was an overlap of one third of the area between two successive pulses. Irradiation took place either in the open atmosphere or in a 10^{-7} torr vacuum. The results did not depend on the ambient environment.

A typical surface morphology after laser radiation is shown in Fig. 8a. The important features are outlined in Fig. 8b for a more clear presentation. Depending on the power level, there are three distinctive regions of interaction:

1. Material evaporation commences at the center of the spot.
2. In the outer peripheral region, there is the formation of a ring area which has higher reflectivity than the normal epilayer and

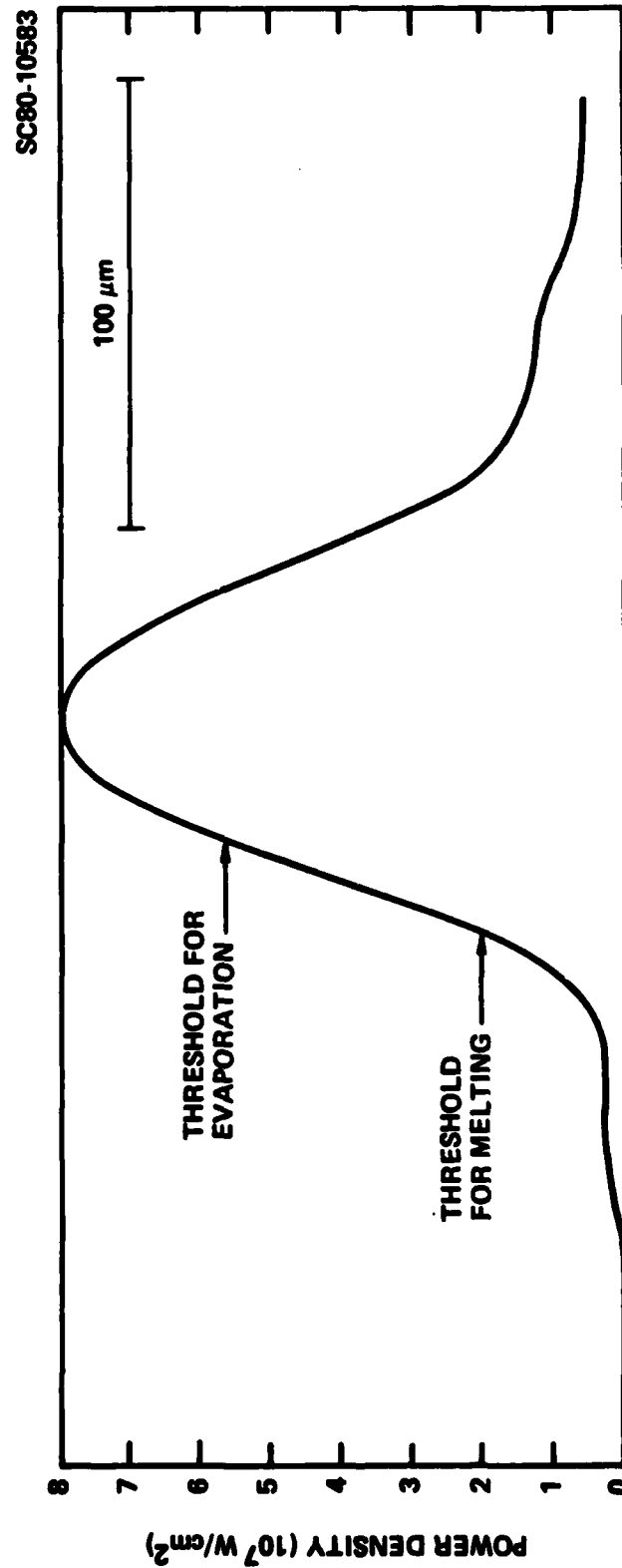
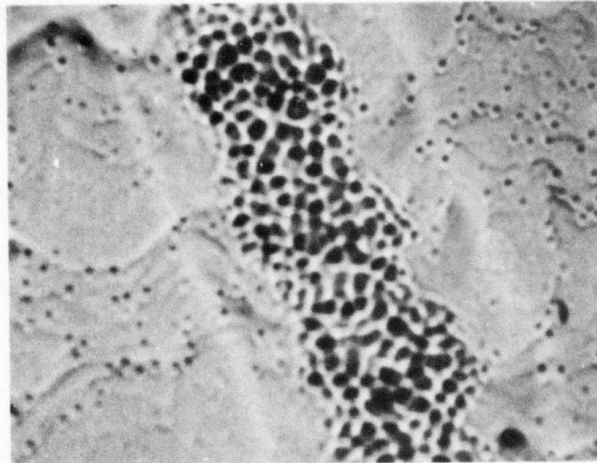


Fig. 7 Laser beam profile.

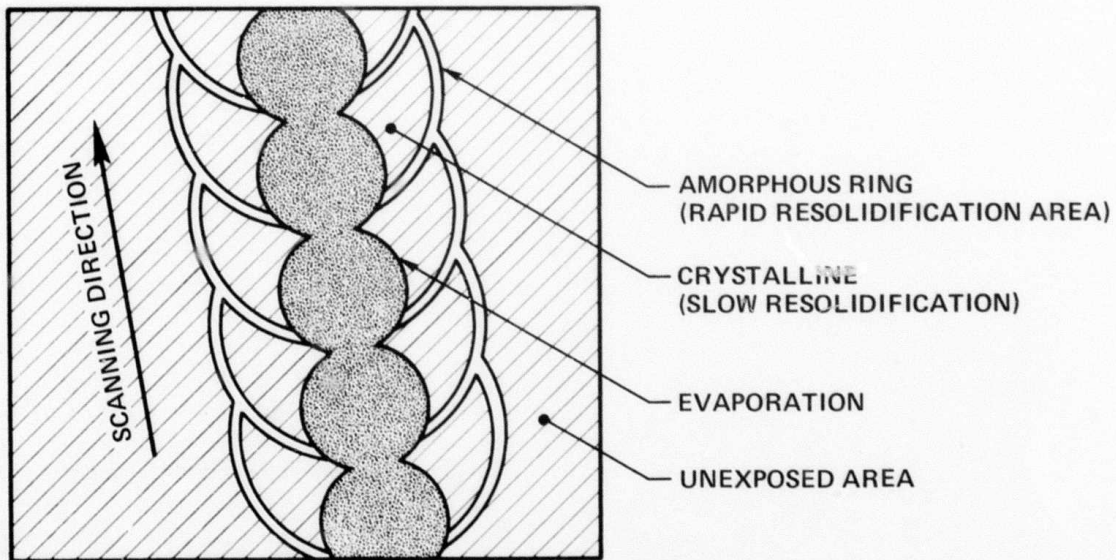


SC80-10584

100 μm



(a)



(b)

Fig. 8 Surface morphology of an epilayer after laser annealing.



SC5202.9SA

hence shows light color. When a train of pulses were scanned of the surface with a slight overlap, the individual rings merge together to form a series of open circles. Their diameters increase in size with higher power density.

3. The area between the above two regions does not show any visible change.

The structure of the surface layer was examined by x-ray topography. Results showed that the central region was highly damaged, whereas the outer region was still single crystal just like the unexposed area. The topograph could not resolve any structural difference in the highly reflective ring area, perhaps due to the insufficient thickness. By correlating the diameter of these regions to the beam profile, we found that a threshold power densities of $6 \times 10^7 \text{ W/cm}^2$ for evaporation and $2 \times 10^7 \text{ W/cm}^2$ for the formation of the highly reflective ring. In both cases, the onsets were very sharp.

One plausible explanation to account for the appearance of the light colored ring area is the formation of an amorphous layer. The mechanism can be described in the following.

When a single crystal HgCdTe surface absorbs a 200 ns laser pulse, its surface temperature rises rapidly. Evaporation takes place in the central area where the power density exceeds $6 \times 10^7 \text{ W/cm}^2$. In the outer region, surface temperature is lower and the surface material can only pass into the liquid state. The boundary of the melt is marked by the highly reflective



SC5202.9SA

ring area. The minimum power requirement is therefore 2×10^7 W/cm². Resolidification takes place after the pulse tails off. The final state is determined by the crystal growth speed and cooling rate. For any semiconductor material, there is always a limiting maximum growth rate μ for crystallization. For example, Spaepen and Turnbull³ have calculated for Ge $\mu = 10^4$ cm/s. The limiting growth rate for HgCdTe will certainly be much slower due to its compositional complexity. If solidification occurs at a faster rate than μ it will be possible for an amorphous solid phase to nucleate first. The melting temperature of amorphous HgCdTe is not known, but it should be lower than the melting point of the crystal structure. If a HgCdTe liquid layer of thickness d is supercooled well below this temperature in a time short compared to d/μ , i.e., $d/\mu \gg t_{\text{cooling}}$, amorphous solid phase can be formed. After the laser pulse has created a circular region of melt, the temperature at edge of the melt will be the lowest and it will be the first to cool down. Therefore, if the condition for amorphous phase formation is to be fulfilled, it must be first fulfilled by the material at the edge of the melt. The formation of amorphous state will be a ring area. The melt thickness can be approximated by the thermal diffusion length:

$$d \approx (2k\tau)^{1/2} \quad (5)$$

where k is the thermal diffusivity and τ is the pulse duration. For HgCdTe, under the present condition, the melt is approximately 0.6×10^{-4} cm thick. A cooling time of 10^{-7} s will yield the maximum crystal growth rate to be: $\mu =$



SC5202.9SA

$(t_{\text{cooling}}/d) = 6 \times 10^2$ cm/s. The actual value will be even smaller, since our mass spectroscopic studies indicate a slower cooling rate. This limiting growth rate is two orders of magnitude slower than that for Ge. In an early study Si also exhibits the formation of an amorphous ring after pulsed heating.⁴ Except such pulses must be very short with duration between 10^{-11} second and 10^{-12} second.

It is worth to point out another interesting feature. When a train of laser pulses scanned across the sample surface, the amorphous ring formed by the previous pulse was recrystallized by the next pulse in the overlapping area. Consequently, a series of open circles was formed. This observation means that the amorphous HgCdTe layer can be recrystallized by 10^{-7} duration laser pulses with the proper power density.

This experiment also provides us with some guidelines in selecting the proper laser power levels for evaporation and in situ annealing.

2.2.4 Results on Laser Annealing

In the previous section, we reported that under proper conditions, amorphous HgCdTe can be recrystallized by pulsed laser irradiation. We deposited a HgCdTe film on a $\langle 111 \rangle$ CdTe substrate at low substrate temperature (130°C). The film did not show any x-ray diffraction pattern indicating its amorphous nature. We then scanned this film with laser pulses for annealing. The laser beam was slightly out of focus, so that the power density at the center was $\sim 8 \times 10^7$ W/cm² and a circular region around it with diameter



SC5202.9SA

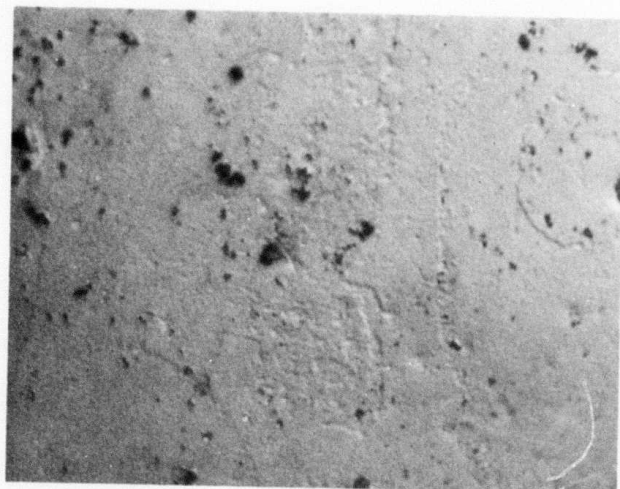
of 0.15 mm had a power density of 1.2×10^7 W/cm² at the edge which is the threshold level for melting. The film was less than 1 μ m thick so the entire thickness would be melted during irradiation. The experiment was carried out in a vacuum at room temperature. Surface morphology of the film before and after the laser irradiation is shown in Fig. 9a,b for comparison. Before laser annealing, the surface was covered with some embedded microparticles and otherwise featureless. After laser annealing, with an exception of a small spot at the center where evaporation took place, all other areas showed a smooth surface. The surface also showed a pattern of triangular lines characteristic of the <111> crystal orientation. Laue x-ray reflection of the annealed film indicated that it was a single crystal in the <111> direction.

In order to examine the origin of these triangular pattern lines, we took the laser annealed sample and etched away the HgCdTe film to expose the CdTe substrate. Under optical microscopic observation, these lines were still clearly visible and extended deep into the substrate surface similar to cracks. We irradiated another piece of CdTe substrate under the identical condition, there was no change on the surface. This was expected since CdTe was transparent at 1.06 μ m wavelength. Therefore, these cracks were caused indirectly by the HgCdTe film above it. One possibility is the direct heat flow from the HgCdTe film into the substrate causing thermal damage. Another explanation is that the radiation power heated up the HgCdTe film to a very high temperature while the CdTe, being transparent, was at a relative low temperature. Therefore, a large thermal mismatch at the interface could result in strains and cracks. This suggests that in the in situ laser

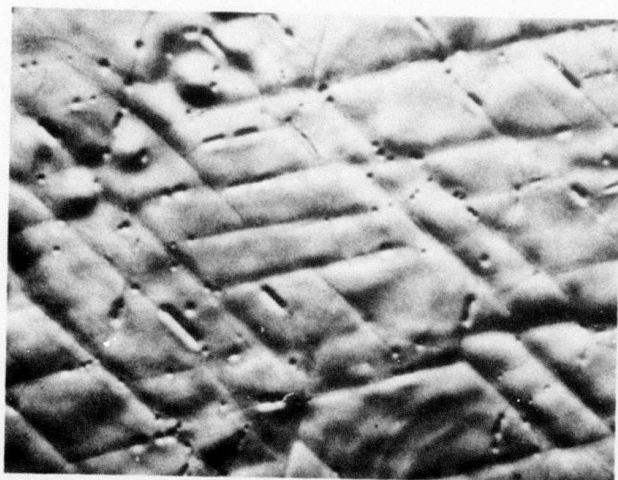


SC80-10585

10 μ



(a) BEFORE LASER ANNEALING



(b) AFTER LASER ANNEALING

Fig. 9 Surface morphology of a laser evaporated film before and after laser annealing.



SC5202.9SA

annealing operation, it would be necessary to raise the substrate temperature as high as possible to avoid this problem.

2.2.5 The Use of Pressed Powder Sample

All previous results were based on the use of bulk HgCdTe for evaporation. Their availability is limited and do not have the quality control from sample to sample. In a recent study of the sputtering deposition of HgCdTe thin film, it was reported the use of homogenized HgTe and CdTe powder as sputtering source.⁵ It yielded results comparable to those using bulk source material. We decided to take the similar approach. HgTe (99.995%) and CdTe (99.999%) from Gellard-Schlesinger Chemical Co. were used. The powdered materials had a particle size of 3 μm or less. Mixtures with a composition of 78% HgTe and 22% CdTe were pressed into 1.3 cm diameter pellets under a pressure of 3 Ton/cm^2 . The pellet was then mounted onto the source holder and the chamber was evacuated. The pellet was outgassed at 110°C in a 10^{-7} torr vacuum overnight before deposition. The outgas procedure was necessary to drive out the air bubbles trapped between the microparticles but it might have side effects since at 110° for a period of many hours HgTe could decompose. Our results showed that even this procedure did not complete outgas the source pellet, splashing problem was still very serious. This was caused by the explosion of the trapped air bubbles. We have purchased a new die for better pellet preparation. The new die is evacuable so the trapped air can be removed during pressing. It can also withstand a much higher pressure of 10 Ton/cm^2 , thus reducing the dead space.



SC5202.9SA

3.0 FUTURE PLANS

Our future plans for the next six months period are:

- 1. To solve the problems of using powder mixture as evaporation source and to grow thick (5 μ m) films.**
- 2. To characterize the films electrically and crystallographically and to use the information for growth optimization.**



SC5202.9SA

4.0 REFERENCES

1. J.F. Ready, Appl. Phys. Lett. 3, 11 (1963).
2. P. Maier-Kormor, Nucl. Inst. and Meth. 167, 73 (1979).
3. S. Spapean and D. Turnbull in Proceedings of Symposium Etch, 1978, Laser-Solid Interaction and Laser Processing (Materials Research Society, Boston).
4. P.L. Liu, R. Yen, N. Bloembergen and R.T. Hodgson, Appl. Phys. Lett. 34 (12), 864 (1979).
5. R.H. Cornely, L. Sundrow, T. Gabara and P. Diodato, IEEE Trans. Elect. Dev, ED-27, 29 (1980).